

High-resolution solid state ^{13}C n.m.r. study of the interpolymer interaction, morphology and chain dynamics of the poly(acrylic acid)/poly(ethylene oxide) complex

Toshikazu Miyoshi*†, K. Takegoshi* and Kunio Hikichi

Section of Structural Bio-Macromolecular Science, Division of Biological Sciences,
 Graduate School of Science, Hokkaido University, 060, Japan
 (Received 24 April 1996; revised 15 July 1996)

The interpolymer interaction, morphology and chain dynamics of the poly(acrylic acid)/poly(ethylene oxide) (PAA/PEO) complex are examined by using ^{13}C CP/MAS n.m.r. methods. By analysing ^{13}C CP/MAS spectra of the complex we conclude that there exist three hydrogen bonding forms for the carboxyl group of PAA, namely: (1) the complex form, interpolymer hydrogen bonding between PEO molecules; (2) the dimeric form, intrapolymer hydrogen bonding within PAA molecules; and (3) the free form, no particular form of hydrogen bonding. The morphology of the complex is investigated by the ^1H spin-lattice relaxation time in the laboratory frame (T_1), and that in the rotating frame ($T_{1\rho}$). We found that the domain sizes of the three hydrogen bonding forms of PAA are less than a few tens of angstroms, and the PAA/PEO complex is miscible on a molecular level. Further, temperature dependence of ^{13}C linewidth (T_2) is examined to study effects of complexation on the molecular motion of the component polymers. The temperatures at which the maximum linewidths are observed for the main chain carbon of PEO and PAA in the PAA/PEO complex are 310 and 362 K, respectively. This indicates that the motional heterogeneity is present in spite of a single T_g for the PAA/PEO complex. Further, we discuss the structural difference between the poly(methacrylic acid)/PEO complex and the PAA/PEO complex. © 1997 Elsevier Science Ltd.

(Keywords: poly(acrylic acid); poly(ethylene oxide); polymer complex)

INTRODUCTION

There has been continuous interest in the structure and the complexation mechanism of poly(methacrylic acid)/poly(ethylene oxide) (PMAA/PEO) and poly(acrylic acid)/poly(ethylene oxide) (PAA/PEO) complexes. In the solution state, it was shown that interpolymer hydrogen bonding occurs between the carboxyl proton of PMAA, PAA and the ether oxygen of PEO and that the hydrophobic interaction between the methyl group of PMAA and the methylene group of PEO makes the PMAA/PEO complex more stable than the PAA/PEO complex^{1–4}.

In the solid state, the physical properties of the polymer complex were examined by various methods such as d.s.c.^{5–7} and stress relaxation⁸. D.s.c. and stress relaxation measurements, however, give different perspectives on the glass transition T_g of the PAA/PEO and PMAA/PEO complexes. Kim *et al.* showed that $T_g = 453$ K of the PMAA/PEO complex differs from those of pure PEO (180 K) and pure PMAA (483 K)⁸. Smith *et al.* showed that the T_g value of the PAA/PEO complex is 278 K, which is close to the average of those of PEO and PAA ($T_g = 373$ K)⁵. These results show that both complexes are homogeneous to a few hundred

angstroms and that motional heterogeneity does not exist in the complexes. Recently, Maunu *et al.* re-examined the T_g values of both complexes. However, they found that it is difficult to obtain the T_g value with sufficient accuracy to yield information on complexation⁶.

High-resolution solid state ^{13}C n.m.r. is a powerful tool for the study of chain dynamics and the structure of polymer mixtures (for a review, see Takegoshi⁹). Recently, we examined the chain dynamics of the PMAA/PEO complex, and showed motional heterogeneity between PMAA and PEO¹⁰. Further, it was shown that two types of hydrogen bonding for the carboxyl group of PMAA exist in the PMAA/PEO complex: hydrogen bonding between the carboxyl group and PEO (the complex form) and hydrogen bonding between the carboxyl group and PMAA (the dimeric form). Spin diffusion experiments showed that the complex is homogeneous on a scale of a few tens of angstroms. An i.r. study also showed that the two kinds of carboxyl group exist in the PMAA/PEO complex⁸. For the PAA/PEO complex, however, an i.r. study indicated that there are three kinds of carboxyl group⁷. These three types of carboxyl group are assigned to (1) those forming interpolymer hydrogen bonds between PAA and PEO (the complex form), (2) those forming intra-hydrogen bonds within PAA molecules (the dimeric form), and (3) those not undergoing hydrogen bonding (the free form).

* Present address: Department of Chemistry, Graduate school of Science, Kyoto University, Kyoto 606-01, Japan

† To whom correspondence should be addressed

In this study, we examine the PAA/PEO complex using ¹³C CP/MAS n.m.r. methods. Firstly, the structure of the carboxyl group is examined by analysing the ¹³C lineshape. Secondly, the miscibility of the PAA/PEO complex is examined by the ¹H spin-lattice relaxation time in the laboratory frame (*T*₁), and that in the rotating frame (*T*_{1ρ}). Lastly, segmental motion of the component polymer in the complex is studied through the ¹³C linewidth (*T*₂). Further, we discuss the structural difference between PMAA/PEO and PAA/PEO complexes.

EXPERIMENTAL

Samples

PEO with an average molecular weight of 20 000 was obtained from Asahidenka, Co. PAA with an average molecular weight of 90 000 was purchased from Aldrich, Co. PAA and PEO were dissolved separately in water (3 wt%), and the pH adjusted to 2.0 by 1 N HCl solution. The PAA and PEO solutions were mixed with different compositions of PAA/PEO: (a) 1/2, (b) 1/1 and (c) 2/1 in monomer units. As soon as the solutions were mixed, white precipitates appeared. After the solutions were left for about 1 day, the precipitates were washed, and dried for 3 days under vacuum at 298 K. The compositions were determined by the ¹H signals of the sample dissolved in dimethylsulfoxide-*d*₆, and are listed in Table 1. Unlike the PMAA/PEO complex whose compositions are independent (1/1) of the mixing ratios¹⁰, the compositions of the PAA/PEO complexes depend on the mixing ratios. We will denote the three complexes (a), (b) and (c).

N.m.r. experiment

The ¹³C n.m.r. experiments were carried out with a JEOL GX-270 spectrometer operating at resonance frequencies of 270 MHz for ¹H and 67.5 MHz for ¹³C. High-resolution solid state ¹³C n.m.r. spectra were obtained by the combined use of high-power proton decoupling (d.d.) and magic angle spinning (MAS). The radiofrequency field strength for both ¹H and ¹³C was about 55.6 kHz. The ¹H decoupling frequency was chosen to be 3 ppm downfield from tetramethylsilane (TMS). A double-bearing aluminium oxide rotor was used at a spinning frequency of 5.5 kHz. The setting of the magic angle was monitored by the ⁷⁹Br n.m.r. spectrum of KBr incorporated in the rotor. The ¹³C chemical shifts were calibrated in parts per million relative to TMS by taking the ¹³C chemical shift of the methine carbon of solid adamantane (29.5 ppm) as an external reference standard. The contact time of cross-polarization (CP) was 500 μs. A shorter CP time of 100 μs was used to observe the spectra of pure PEO, and to measure the rotating frame spin-lattice relaxation times (*T*_{1ρ}) for all the samples at 310 K. Variable-temperature measurements were accomplished by using a JEOL MVT temperature controller with an accuracy of 1 K.

Table 1 The compositional ratios of the PAA/PEO complexes with various mixing ratios

Complex	Mixing ratio of PAA/PEO	Compositional ratio of PAA/PEO
(a)	1/2	1.0/1.2
(b)	1/1	1.0/1.0
(c)	2/1	1.4/1.0

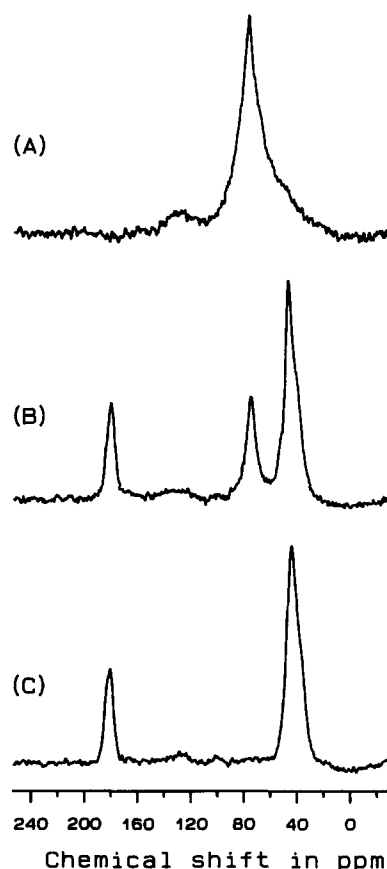


Figure 1 ¹³C CP/MAS spectra of the PAA/PEO complex at 310 K: (A) pure PEO, (B) complex (b) and (C) pure PAA

RESULTS AND DISCUSSION

Hydrogen bonding structure

Figure 1 shows the ¹³C CP/MAS n.m.r. spectra of pure PEO, the PAA/PEO complex (b), and pure PAA at 310 K. The line width of the ¹³C peak of pure PEO is very broad. This broadening has been attributed to the interference of ¹H decoupling with the molecular motion of PEO in the crystalline phase¹¹. For pure PAA, two distinct peaks are observed: one appears at around 40 ppm and the other at 181 ppm. The former is the methine and methylene carbons, and the latter is the carboxyl carbon. For the complex, two spectral changes are appreciable. One is the decrease of the linewidth of PEO. Similar line narrowing of PEO upon complexation or blending has been observed for the PMAA/PEO complex¹⁰ and poly(vinyl phenol) (PVPh)/PEO blends¹¹. It has been interpreted as the destruction of the crystalline phase of PEO. The other spectral change is the upper-field shift (181 → 179 ppm) of the carboxyl carbon of PAA upon complexation. This shift is attributed to the formation of hydrogen bonds upon complexation.

In order to further examine the hydrogen bonding structure in the complex, we obtained several spectra at various temperatures. Figure 2 shows three typical spectra of the carboxyl region of the complex (b). At low temperatures below 278 K, a triplet signal was observed. A similar lineshape was also observed for complexes (a) and (c) (Figure 3). It is expressed by a sum of three Gaussian lineshape functions (Figure 4). The best-fitted parameters are given in Table 2. The best-fitted chemical shift values for the three peaks are almost

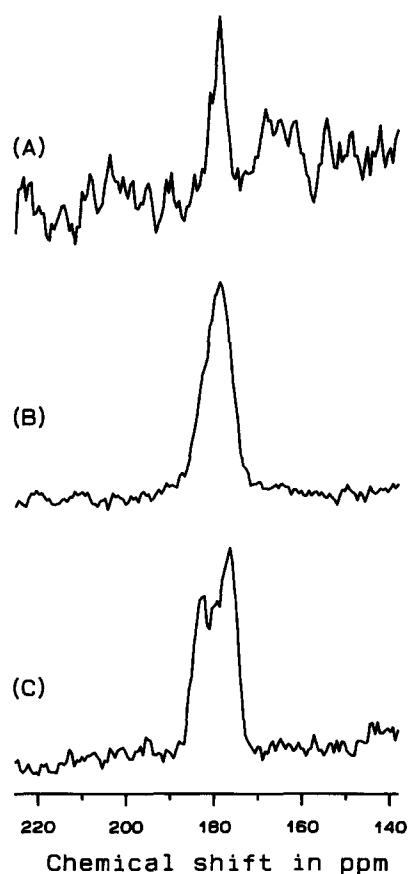


Figure 2 ¹³C CP/MAS spectra of the carboxyl carbon in the PAA/PEO complex (b) at various temperatures: (A) 386 K, (B) 310 K and (C) 234 K

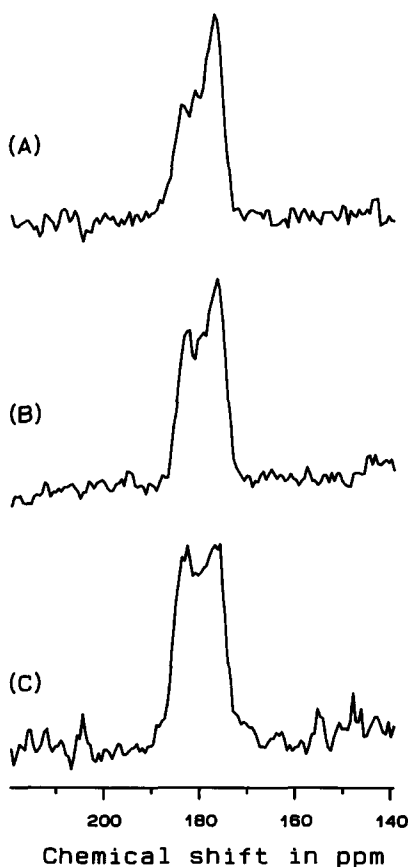


Figure 3 ¹³C CP/MAS spectra of the carboxyl carbon in the PAA/PEO complexes at 234 K: (A) complex (a), (B) complex (b) and (C) complex (c)

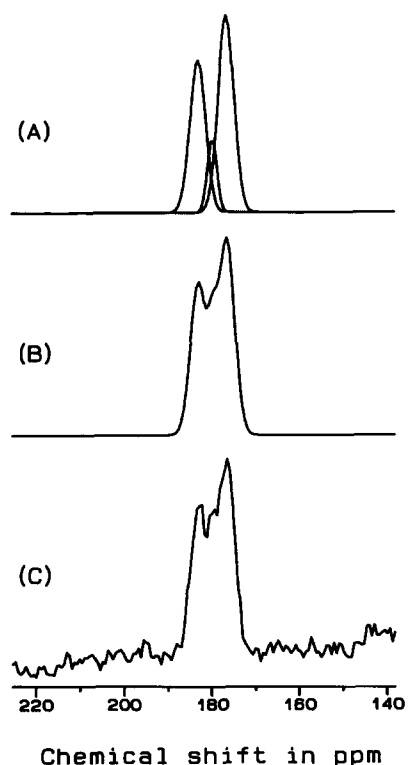


Figure 4 ¹³C CP/MAS spectra of the carboxyl carbon in the PAA/PEO complex (b) at 234 K: (A, B) simulated and (C) experimental

constant for complexes (a)–(c). The peak at 176 ppm has the largest intensity, and it decreases with decreasing PEO content ((a) → (c)). Therefore, this peak is assigned to carboxyl groups involved in interpolymer hydrogen bonding between PAA and PEO (the complex form). The peak intensity at 183 ppm is the next largest, and its intensity decreases with increasing PEO content. Thus, this peak is assigned to carboxyl groups undergoing intrahydrogen bonding within PAA (the dimeric form). The peak at 180 ppm is much smaller than the above-mentioned two peaks. Further, the chemical shift value is close to that of pure PAA in methanol solution (179 ppm). Therefore, the peak at 180 ppm is assigned to carboxyl groups that form no particular hydrogen bonds in the solid. These latter carboxyl groups may correspond to ‘the free form’ carboxyl group postulated by the i.r. study⁷. Thus, we shall denote this form of carboxyl group the free form. However, we do not mean that this carboxyl group is ‘free’ from any hydrogen bonding involvement.

A similar lineshape splitting upon complexation has been observed for the PMAA/PEO complex¹⁰. For this complex, the lineshape has been expressed as a sum of two peaks: one is the dimeric form appearing at lower field (187 ppm) and the other is the complex form at higher field (180 ppm). It was noted that the tendency of the higher-/lower-field shift of the complex/dimeric form was similar to that found for the PAA/PEO complex.

At higher temperatures above 310 K, we observed a single peak at 179 ppm (Figure 2B). Further increase in temperature brings about line narrowing, and the intensity of the peak decreases (Figure 2A). However, the chemical shift value of the peak is constant (179 ppm) in the region of 310–386 K.

This spectral change may be attributed either to an increase in the free form or to motional averaging among

Table 2 The relative intensities, the best-fitting chemical shifts and linewidths for the ¹³C peaks of the three forms carboxyl carbons in the PAA/PEO complexes^a

	Complex form	Dimeric form	Free form
<i>Complex (a)</i>			
Relative intensity (%)	63 ± 7	31 ± 7	6 ± 8
Chemical shift (ppm)	176.5 ± 0.2	183.0 ± 0.3	179.4 ± 0.2
Linewidth (Hz)	326.3 ± 25.4	285.3 ± 44.5	109.4 ± 63.1
<i>Complex (b)</i>			
Relative intensity (%)	53 ± 9	38 ± 7	9 ± 10
Chemical shift (ppm)	176.2 ± 0.4	182.8 ± 0.3	179.4 ± 0.4
Linewidth (Hz)	312.5 ± 37.0	296.9 ± 47.5	152.2 ± 116.9
<i>Complex (c)</i>			
Relative intensity (%)	40 ± 19	41 ± 16	19 ± 30
Chemical shift (ppm)	176.3 ± 0.4	183.1 ± 0.4	179.5 ± 0.7
Linewidth (Hz)	312.2 ± 66.3	312.5 ± 58.5	296.8 ± 315.3

^a Errors are 2.5σ

the three peaks. The former case, however, is negated because the increment of the free form would lead to the phase separation, which was not observed in the ¹³C CP/MAS spectra below 386 K. Further, the spectral change is facile and reversible on decreasing the temperature. The reversible process of the phase separation may take a longer time. Thus, we attribute this spectral change to the latter case.

Here, we neglect the small amount of the free form, and treat the problem as a two-site exchange. The chemical shift value at a fast exchange limit can be expressed as

$$\sigma_{av} = \rho_A \sigma_A + \rho_B \sigma_B \quad (1)$$

where the chemical shifts of the complex form and the dimeric form are represented as σ_A and σ_B, respectively. ρ_A and ρ_B are the relative intensities of the two forms. The best-fitting parameters for complex (b) in Table 2 are used to calculate σ_{av}. In consequence, the calculated chemical shift σ_{av} is 179 ppm, and is in good agreement with the observed value (179 ppm). Thus, at higher temperatures, a fast exchange between the carboxyl groups occurs.

For pure PAA at 310 K, we observe a singlet at 181 ppm. This value may also be understood as an average between the dimeric form and the free form. However, since the T_g of pure PAA (373 K) is much higher than the observed temperature (310 K), the lineshape is not a motional averaged one but a static superposition of the two peaks.

Miscibility

In this section we examine the miscibility of the PAA/PEO complex by using the ¹H spin-lattice relaxation time in the laboratory frame (T₁) and that in the rotating frame (T_{1ρ}). We measured the ¹H T₁ at 310 K, and ¹H T_{1ρ} at 310 and 234 K. The observed ¹H T₁ and T_{1ρ} times are listed in Table 3. The relaxation time of PAA was obtained through the main-chain peak at 310 K. To examine the heterogeneity of structure in the complex, we analysed the carboxyl peak at 234 K.

For the ¹H T₁ measurement, the T₁ values of pure PAA and PEO are 1.30 and 3.68 s, respectively. For

complexes (a) and (c), the T₁ values of the component polymers agree with each other within experimental error, showing that the T₁ relaxation processes of the component polymers are averaged by a fast spin diffusion between them. This shows that PAA and PEO are miscible in the complexes on a scale of 200–300 Å.

For the ¹H T_{1ρ} measurements at 310 K, a single relaxation time was obtained for pure PAA. On the other hand, a double exponential decay was observed for pure PEO. The two T_{1ρ} values (> 5 and 0.20 ms) have been attributed to the amorphous and crystalline phases of PEO, respectively^{10–12}. For the complexes, non-single exponential decay curves are observed for both PAA and PEO (Figure 5). In order to analyse the observed decay curves, we treat the spin system as two dipolar-coupled two-spins A (PAA) and B (PEO). The dynamics of the magnetizations during the T_{1ρ} relaxation process may be given by the following equations¹³:

$$-\frac{dM_A}{dt} = (K_A + f_B + f_B K_C)M_A - f_A K_C M_B \quad (2a)$$

$$-\frac{dM_B}{dt} = (K_B + f_A K_C)M_B - f_B K_C M_A \quad (2b)$$

Table 3 The proton spin-lattice relaxation time in the laboratory frame (T₁) and in the rotating frame (T_{1ρ}) of pure PAA, pure PEO, and the PAA/PEO complexes (a) and (c)^{a,b}

	310 K T ₁ (s)	310 K T _{1ρ} (ms)	234 K T _{1ρ} (ms)
<i>Pure</i>			
PAA	1.30 ± 0.10	2.21 ± 0.20	5.20 ± 0.20
PEO	3.68 ± 1.19	0.20 ± 0.03	20.70 ± 1.61
<i>Complex (a)</i>			
PAA	1.07 ± 0.05	1.67 ^b	3.52 ± 0.27 (complex) 3.49 ± 0.45 (dimeric)
PEO	1.10 ± 0.10	0.37 ^b	3.66 ± 0.20
<i>Complex (c)</i>			
PAA	1.18 ± 0.04	2.50 ^b	4.35 ± 0.40 (complex) 4.55 ± 0.40 (dimeric)
PEO	1.28 ± 0.09	0.77 ^b	4.65 ± 0.18

^a Errors are 2.5σ

^b Values obtained using equation (2)

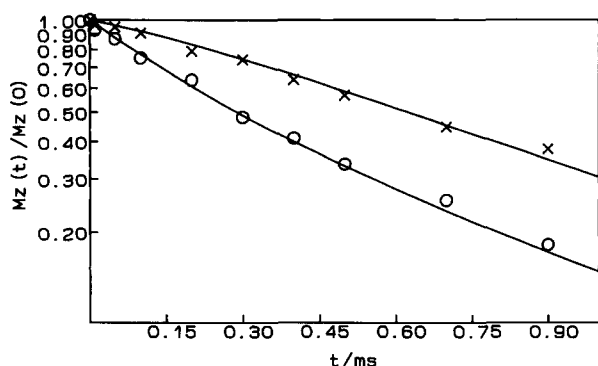


Figure 5 The observed ¹H *T*_{1ρ} decay curves for PAA (×) and PEO (○) in complex (a). The solid lines were calculated using equation (2) with parameters of *K*_A = 0.6 × 10³ s⁻¹, *K*_B = 2.7 × 10³ s⁻¹ and *K*_C = 2.2 × 10³ s⁻¹

where *M*_{*i*}, *f*_{*i*} and *K*_{*i*} denote the magnetization, the ¹H mole fraction and the intrinsic relaxation for the polymer (*i* = A or B), respectively. *K*_C is the interpolymer cross-relaxation rate (the spin diffusion rate). The solid lines in Figure 5 are the best-fitted lines with the parameters listed in Table 3. The spin diffusion rates (*K*_C) for complexes (a) and (c) are 2.2 × 10³ and 1.7 × 10³ s⁻¹, respectively. It is shown that the spin diffusion is too slow to average the fast *T*_{1ρ} processes of the component polymers. This slow spin diffusion can be explained by a heterogeneous structure¹³ or a fast molecular motion^{10,14}.

PEO is a highly mobile polymer, and the *K*_B value (*T*_{1ρ}⁻¹) of PEO in the complex is close to the inverse of the *T*_{1ρ} minimum value of amorphous phase of pure PEO (0.5 m)¹². This indicates the fast molecular motion of PEO in the complex, and it is reasonable to conclude that this fast motion averages the ¹H-¹H dipole interactions between PAA and PEO to some extent, resulting in the incomplete spin diffusion.

In order to suppress the motional effect, we measured ¹H *T*_{1ρ} at 234 K. At this temperature, only one *T*_{1ρ} component was observed for pure PEO^{10,12}. For the complexes, a single exponential decay curve was observed for both PAA and PEO, and the *T*_{1ρ} value of PEO is similar to those of PAA for the two complexes studied. This shows that PAA and PEO are miscible on the scale of 20–30 Å. Further, the *T*_{1ρ} value of the complex form agrees with that of the dimeric form for complexes (a) and (c) (Table 3). This shows that the complex form and the dimeric form are in close proximity and may co-exist in the same PAA chain.

Molecular motion

In the previous section, the fast molecular motion of PEO is suggested by the short ¹H *T*_{1ρ} value at 310 K. In this section, we examine the main-chain motion of each component polymer in the complex through the resolved ¹³C peaks. Figure 6 shows the ¹³C CP/MAS spectra of complex (b) at various temperatures under ¹H dipolar decoupling. The spectra below 234 K are independent of temperature (Figure 6C). With increasing temperature, the linewidth of PEO shows broadening, and reaches the maximum broadening at 310 K (Figure 6B). Further increase in temperature brings about the line narrowing of PEO, and line broadening of PAA occurs. At 362 K, the linewidth of the PAA main-chain peak reaches its maximum (Figure 6A).

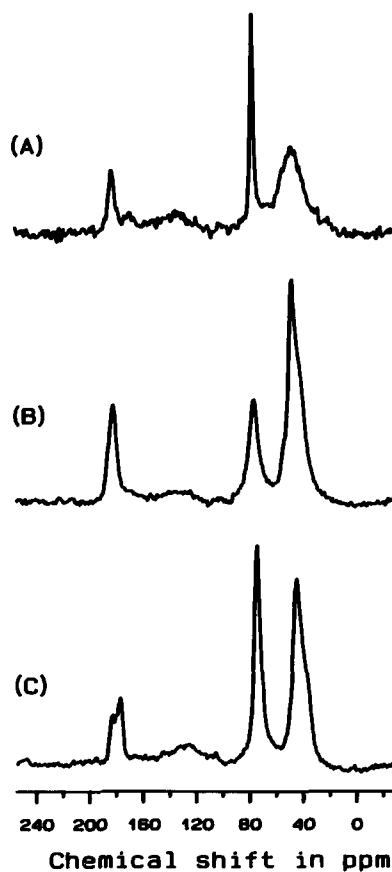


Figure 6 ¹³C CP/MAS n.m.r. spectra of the PAA/PEO complex (b) at various temperatures: (A) 362 K, (B) 310 K and (C) 234 K

The observed linewidths of PEO in the PAA/PEO complex are plotted against temperature in Figure 7. This line broadening/narrowing is attributed to the interference between molecular motion and the ¹H decoupling. When the motional frequency is equal to the ¹H decoupling frequency, the interference effect is at a maximum, leading to the maximum linewidth^{15,16}. The observed different maximum broadening temperatures for PAA and PEO in the complex shows that the motional heterogeneity is present in spite of the single *T*_g for the PAA/PEO complex.

The temperature dependence of the ¹³C linewidth of a polymer under high-power ¹H decoupling may be expressed by the following empirical equation¹⁷:

$$\delta = \delta_0 + \delta_1 \left(\frac{2}{\pi} \right)^{-1} \tan[\alpha(T_0 - T)] + \lambda M_2 \frac{\tau}{1 + \omega_1^2 \tau^2} \quad (3)$$

where the first term represents the intrinsic linewidth arising from various static line broadenings. The second term describes the motional averaging of the distribution of the isotropic chemical shift. Arctangent dependence was assumed, and α describes the steepness of the narrowing. *T*₀ is the characteristic temperature designating the onset of molecular motion. The third term represents the linewidth arising from the ¹³C-¹H dipole interaction^{15,16}. *M*₂ represents the powder average of the second moment of the ¹³C-¹H dipolar interaction. λ is a reduction factor of the second moment (0 < λ < 1); for isotropic motion $\lambda = 1$. λ decreases as the motion becomes more anisotropic. τ and ω_1 are a correlation time and ¹H decoupling frequency, respectively. It is

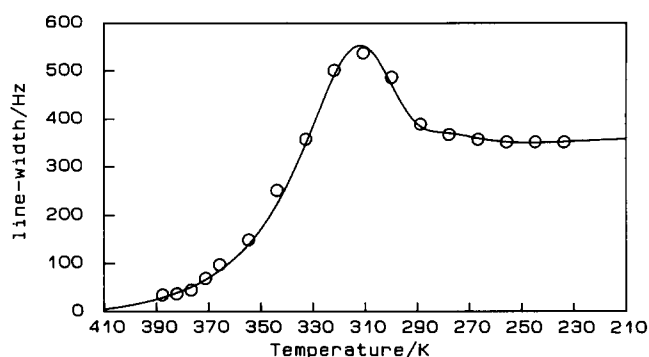


Figure 7 The observed ¹³C linewidth of the CH₂ carbon of PEO in the PAA/PEO complex (b) at various temperatures. The solid line is the best-fitted one obtained using equations (3) and (4)

assumed that the correlation time has an Arrhenius-type dependence on temperature:

$$\tau = \tau_0 \exp\left(\frac{E_a}{RT}\right) \quad (4)$$

where E_a is the activation energy and τ_0 is the correlation time at infinite temperature. A more detailed explanation of equations (3) and (4) may be found in Takegoshi and Hikichi¹⁷. We fitted the linewidth of PEO to equations (3) and (4), and the best-fitted line is shown as the solid line in Figure 7. The best-fitted parameters are listed in Table 4.

For comparison, we also re-examined the observed temperature dependent linewidth of PEO in the PMAA/PEO complex, and the best-fitted parameters are collated in Table 4¹⁰. It is noted that the T_0 value of PEO in the PAA/PEO complex is very similar to that of the PMAA/PEO complex. Further, for the PVPPh/PEO = 58/42 blend, a similar value was obtained ($T_0 = 272$ K)¹⁸. Therefore, the T_0 value of PEO in the hydrogen-bonded blend/complex is independent of the counterpart polymer. However, the E_a and λ values (10 kcal mol⁻¹ and 0.136) of PEO in the PAA/PEO complex are much larger than those of PEO in the PMAA/PEO complex (6.7 kcal mol⁻¹ and 0.079)¹⁰. This shows that PEO motion in the PMAA/PEO complex is more restricted and anisotropic than that in the PAA/PEO complex.

For PAA in the complex, the maximum broadening is observed at 362 K. On the other hand, for PMAA in the complex, the line broadening of PMAA is not observed below 383 K. This shows that the motional heterogeneity between PAA and PEO is smaller than that between PMAA and PEO. This leads us to envisage that the complex form is more stable in the PAA/PEO complex than in the PMAA/PEO complex. This may explain the

Table 4 The best-fitting parameters of the CH₂ linewidth of PEO in the PAA/PEO and PMAA/PEO complexes^a

Parameter	PAA/PEO	PMAA/PEO ^b
E_a (kcal mol ⁻¹)	10.0 ± 1.8	6.7 ± 1.0
λ	0.136 ± 0.026	0.079 ± 0.026
$\tau_0 \times 10^{-13}$ (s)	2.3 ± 6.1	480.0 ± 834.9
T_0 (K)	278.6 ± 12.5	270.4 ± 13.8
δ_0 (Hz)	176.3 ± 29.9	213.0 ± 20.5
δ_1 (Hz)	205.7 ± 39.8	138.3 ± 20.2
α	0.079 ± 0.029	0.069 ± 0.054

^a Errors are 2.5 σ

^b From Miyoshi et al.¹⁰

observed temperature dependence of the hydrogen bonding structure in both complexes. At low temperatures (> 234 K), two kinds of carboxyl group (the complex form and the dimeric form) exist in the PMAA/PEO complex¹⁰, while three kinds of carboxyl group (the complex form, the dimeric form and the free form) exist in the PAA/PEO complex. On increasing the temperature to above 310 K, the complex form is destroyed for the PMAA/PEO complex and rearranged into the dimeric form among PMAA molecules¹⁰. For the PAA/PEO complex, the complex form is as stable as the dimeric form, and exchange of hydrogen bonding occurs at higher temperatures.

SUMMARY

¹³C CP/MAS n.m.r. spectra of the PAA carboxyl region show that there exist three forms of hydrogen bonding in the PAA/PEO complex, namely: (1) the complex form, interpolymer hydrogen bonding between PEO molecules; (2) the dimeric form, intrapolymer hydrogen bonding among PAA molecules; and (3) the free form, no particular form of hydrogen bonding. ¹H T_1 and $T_{1\rho}$ results indicate that PAA and PEO are miscible, and the different types of hydrogen bonding are distributed in the complex on a scale of 20–30 Å. Further, temperature dependence of the ¹³C linewidth measurement leads us to conclude that there is a motional heterogeneity between PAA and PEO in spite of mixing on a 20–30 Å scale.

ACKNOWLEDGEMENT

This work was supported by a grant from the Shimadzu Science Foundation.

REFERENCES

- Ikawa, T., Abe, K., Honda, K. and Tsuchida, E., *J. Polym. Sci., Polym. Chem., Part A* 1975, **13**, 1505.
- Osada, Y. and Sato, M., *J. Polym. Sci., Polym. Lett., Part C* 1976, **14**, 124.
- Bailey, F. E., Lundberg, R. D. Jr and Callard, R. W., *J. Polym. Sci., Polym. Chem., Part A* 1964, **2**, 845.
- Antipina, A. D., Baranovskii, V. Y., Papisov, I. M. and Kavanov, V. A., *Vyskomol. Soedin. Ser (A)*, 1972, **14**, 941.
- Smith, L. K., Winslow, A. E. and Petersen, D. E., *Ind. Eng. Chem.* 1959, **11**, 1363.
- Maunu, S. L., Kinnunen, J., Sojiamo, K. and Sunsholn, F., *Polymer* 1993, **34**, 1141.
- Xinya, L. and Weiss, R. A., *Macromolecules* 1995, **28**, 3022.
- Kim, H. J. and Tonami, H., *Kobunshi Ronbunshuu* 1978, **35**, 395.
- Takegoshi, K., *Annu. Rep. NMR Spectrosc.* 1995, **30**, 97.
- Miyoshi, T., Takegoshi, K. and Hikichi, K., *Polymer* 1996, **26**, 11.
- Zhang, X., Takegoshi, K. and Hikichi, K., *Macromolecules* 1992, **25**, 2336.
- Johansson, A. and Tegenfeldt, J., *Macromolecules* 1992, **25**, 4718.
- Stejskal, E. O., Schaefer, J., Sefik, M. D. and McKay, R. A., *Macromolecules* 1981, **14**, 275.
- Asano, A., Takegoshi, K. and Hikichi, K., *Polymer* 1994, **39**, 5630.
- Vanderhart, D. L., Earl, W. P. and Garroway, A. N., *J. Magn. Reson.* 1981, **44**, 361.
- Rothwell, W. P. and Waugh, J. S., *J. Chem. Phys.* 1981, **74**, 2721.
- Takegoshi, K. and Hikichi, K., *J. Chem. Phys.* 1991, **94**, 3200.
- Zhang, X., Takegoshi, K. and Hikichi, K., *Macromolecules* 1993, **26**, 2198.